CERTIFICATION FRAMEWORK: LEAKAGE RISK ASSESSMENT FOR CO2 INJECTION AT THE MONTEZUMA HILLS SITE, SOLANO COUNTY, CALIFORNIA

Curtis M. Oldenburg1, Preston Jordan1, Alberto Mazzoldi1, Jeff Wagoner4, Steven L. Bryant2, Jean-Philippe Nicot3

1 Lawrence Berkeley National Laboratory, 2 University of Texas, Austin, 3 Bureau of Economic Geology, University of Texas, 4 Lawrence Livermore National Laboratory

DOE Contract No.: DE-FC26-05NT42593

Contract Period: October 1, 2005 - May 11, 2011

Certification Framework: Leakage Risk Assessment for CO_2 Injection at the Montezuma Hills Site, Solano County, California

Curtis M. Oldenburg[1], Preston Jordan[1], Alberto Mazzoldi[1],
Jeff Wagoner[4], Steven L. Bryant[2], Jean-Philippe Nicot[3]

[1]Lawrence Berkeley National Laboratory, [2]CPGE, University of Texas, Austin,
[3]Bureau of Economic Geology, University of Texas, [4]Lawrence Livermore National Laboratory

1 Introduction

WESTCARB and C6 Resources are partners in a CO_2 injection project in the Montezuma Hills, 80 km (50 mi) northeast of San Francisco, CA. Through a phased process that involves drilling an appraisal well and injecting CO_2 on a small-scale, along with thorough analysis of data and modeling of the system, the goal of the project is to assess the deep geologic formations in the area for Geologic Carbon Sequestration (GCS), and if favorable, inject CO_2 currently emitted to the atmosphere from nearby refinery facilities at industrial scales on the order of 1 million tons of CO_2 per year. The deep geology at the site is considered very favorable for GCS by virtue of the numerous sandstone formations which are potentially capable of storing large amounts of CO_2 and which are vertically separated by thick shale formations that prevent CO_2 from migrating upward. This general geologic environment is a proven trap for natural gas over geologic time as evidenced by the nearby Rio Vista Gas Field. Assuming step-by-step progress through the various stages, the Montezuma Hills project will involve drilling an appraisal well to over 3 km (10,000 ft) depth, carrying out a small-scale evaluation injection of 6,000 tons of CO_2, and evaluation of the feasibility of developing the site for a large-scale injection (e.g., 1 million tons of CO_2), and further consideration of the site for an industrial-scale GCS operation (e.g., 0.75 million tons CO_2/yr for 25 years).

Because GCS is not widely carried out either in the U.S. or abroad, there is very little experience upon which to base estimates of performance of GCS systems. In the absence of a long track record, leakage risk assessment methods are needed to address concerns by the various stakeholders about the effectiveness of CO_2 trapping and the environmental impacts resulting from CO_2 injection. For the last two years, investigators at the Lawrence Berkeley National Laboratory (LBNL), The University of Texas at Austin (UT), and the Texas Bureau of Economic Geology (TBEG) have been developing a framework called the Certification Framework (CF) for estimating CO_2-leakage risk for GCS sites (Oldenburg et al., 2009). Risk assessment methods such as the CF rely on site characterization, predictive models, and various methods of addressing the uncertainty inherent in subsurface systems. A brief outline of the methods used in the CF is provided in Appendix A. This report presents a discussion of leakage risk issues for the Montezuma Hills project and an outline of the research that needs to be done to carry out a leakage risk assessment by the CF approach.

C6 Resources has already gathered and synthesized a large amount of data and information on the Montezuma Hills site to examine the feasibility of injecting CO_2 at the site. In this case study discussion and research outline, we focus on public data and information that are important

from the perspective of CO_2 and brine leakage risk assessment. For understandability, inevitably some overlap with information already collected will occur, but our emphasis is on data and interpretations relevant to leakage risk assessment that apparently have not previously been considered in detail by C6 or WESTCARB related to vulnerable entities and potential risk mitigation. For example, we discuss the shallow aquifers, surface water, potential for pressure impact on natural gas resources, and the significance of historical natural gas seepage. As for risk mitigation, winds in the area are a favorable mitigating factor relative to surface leakage due to their ability to disperse CO_2 ground plumes. Note that some of the information and text presented here is taken directly from an LBNL report two of us (Oldenburg and Jordan) contributed to several years ago (Oldenburg et al., 2003), and will be indicated as such.

2 Site Description

2.1 Surface and Climate

The Montezuma Hills are immediately north and west of the Sacramento River in the southwestern part of the Sacramento Valley, CA (Figure 1). Shown in Figure 1 is the location of the proposed appraisal well site 5 km (3 mi) north of the Sacramento River. The Montezuma Hills cover an area of approximately 120 km^2 (45 mi^2) and consist of grassy rounded hills separated by numerous ephemeral and some perennial stream valleys with relief averaging 45-60 m (150-200 ft). The Montezuma Hills are bordered on the west by low-lying tidal wetlands and sloughs, to the north by grassland plains, and to the east and south by the Sacramento River. South and east of the Sacramento River are sub-sea level islands that have been drained and diked off from water channels for agriculture. The Rio Vista Gas Field spans either side of the Sacramento River near the town of Rio Vista, which lies along the Sacramento River along the eastern boundary of the Montezuma Hills. The Montezuma Hills are mostly used for grazing lands and agriculture, rural and semi-rural residential use, and wind power generation. Climate in the area is Mediterranean with warm and dry summers and cool winters. The most significant aspect of the climate for CO_2 leakage risk is the winds, which are relatively strong and steady at this location as discussed next.

Figure 1. Proposed appraisal well site (N 38°06'59.12", W 121°50'18.28"), elev. approx. 80 m (250 ft), in the Montezuma Hills north of the Sacramento River.

2.2 Winds

Winds in the area are favorable for power generation, and the Montezuma Hills is the location of hundreds of large wind turbines. Because winds are a mitigating factor for surface CO_2 release through their ability to disperse surface leakage of CO_2, we present in Figure 2 a quantitative assessment of winds from nearby Twitchell Island. This figure, from Oldenburg et al. (2003), shows a five-year time series (06-11-97 to 06-12-03) of hourly wind speed and direction measurements at the DWR meteorological station on Twitchell Island in the form of a wind rose. In Figure 2, the radial spokes indicate the direction the wind is coming from, the concentric circles are contours of the percentage of time (in 10% intervals) that the wind blows from the given direction, the thickness of the bar on the spokes indicates the wind speed, and the numbers at the end of the spokes are the total percentage time that the wind blows from the given direction. Over the measurement averaging time of 1 hour, there were no calms recorded. Figure 2 shows that the dominant wind direction is from the west to west-southwest (i.e., percent occurrence = 29.44 + 24.53 = 54%). The mean and standard deviation of the corresponding wind speed time series were 3.4 and 2.0 m s^{-1} (7.5 and 6.6 mph), respectively. The dominant wind directions during the spring (March-May), summer (June-August) and a portion of the fall (September-October) are from the west to west-southwest. However, from November to February, dominant wind directions are highly variable. The highest (4.8 m s^{-1} (10.6 mph)) and lowest (2.6 m s^{-1} (5.7 mph)) mean wind speeds were observed during summer and winter months, respectively, while intermediate mean wind speeds were observed during spring and fall months (3.7 and 2.9 m s^{-1} (8.1 and 6.4 mph), respectively).

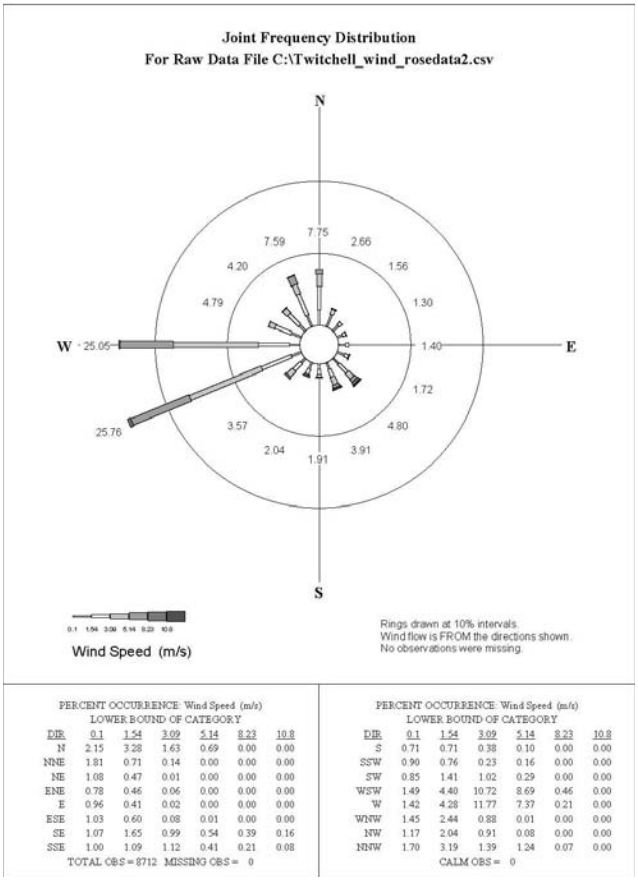

Figure 2. Wind rose for Twitchell Island, CA, located just across the Sacramento River from the Montezuma Hills, south of Rio Vista, CA.

2.3 Natural Gas Seepage

Historical surface natural gas seepage is well documented in California with numerous seeps located in Solano County (e.g., http://geomaps.wr.usgs.gov/seeps/). Early discovery wells at the Rio Vista Gas Field were located near natural gas seeps (Johnson, 1990). The main source of information for hydrocarbon seepage in the area is the public report TR26 by the California Division of Oil & Gas (1987). Chapter 3 of TR26 consists of a long table that identifies and locates 543 onshore oil and gas seeps in California, with several in Solano County in the lands north and northwest of the Montezuma Hills as shown in Figure 3.

The closest mapped historical seeps to the Montezuma Hills are numbered in the TR26 report and shown by the red triangles in Figure. 3. These historical mapped seeps are located in fenced, low-lying agricultural (alfalfa) and/or grazing lands (goats and cattle) with minimal topography. Based on a reconnaissance field trip by three LBNL investigators on March 18, 2009, there does not appear to be any natural gas seepage or associated springs or plant stress in these areas. We concluded from our field reconnaissance and discussions with local landowners that the historical seeps are no longer active. We did observe an abandoned exploration well (locally known as the artesian well) that continuously bubbles water and natural gas in the Denverton, Calif., 7.5 minute quadrangle, in Section 12, along Nurse Slough Rd. (Figure 4). We do not know the depth and other information about this well.

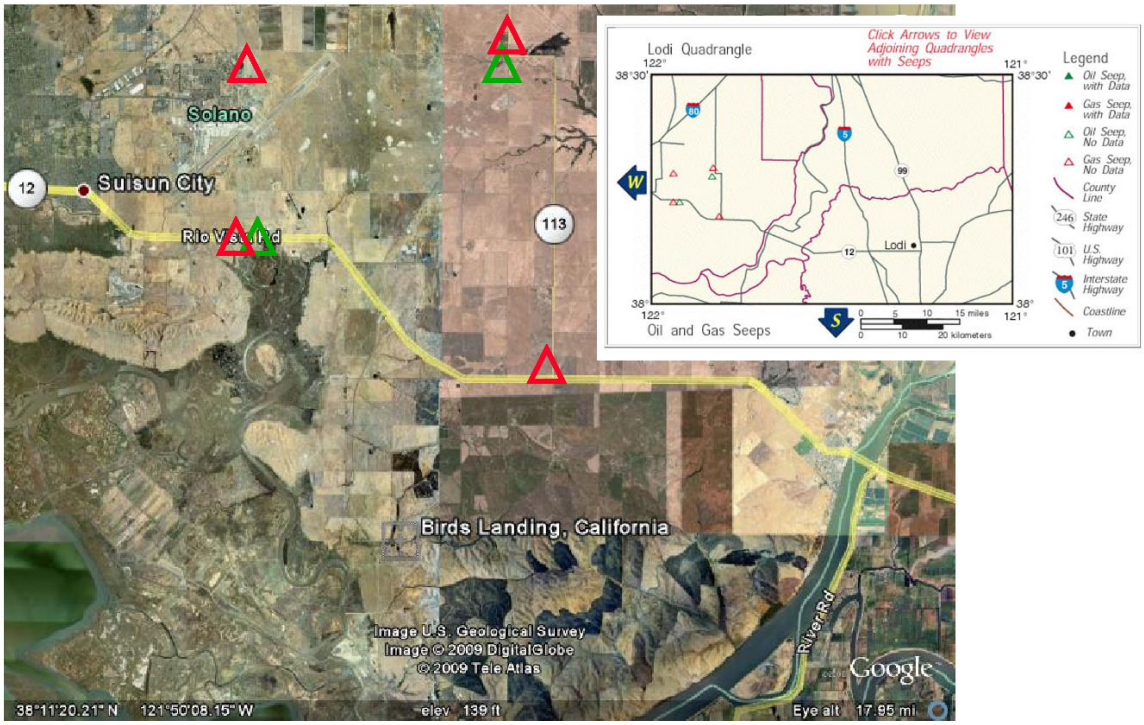

Figure 3. Location map of Solano County seeps from the USGS Seeps webpage (http://geomaps.wr.usgs.gov/seeps/) and transcribed onto a GoogleEarth image.

Figure 4. Photograph of the Nurse Slough Rd. abandoned artesian well with natural gas bubbles and foam at the open well head.

2.4 Surface water

The Montezuma Hills drain predominantly to the southeast to the Sacramento River. The perennial streams in the Montezuma Hills occupy some of these drainages. Minor seasonal streams drain the margins of the hills to the north and west. Extensive wetlands and slough channels cover much of the area between diked-off islands developed for agriculture. The Sacramento River is a major river in California with average flow rate estimated from November 1983 to November 1984 to be 1000 m^3 s^{-1} (35000 ft^3 s^{-1}) (Ota et al., 1986). The mean winter (December-February), spring (March-May), summer (June-August), and fall (September-November) flow rates were estimated to be 2180, 629, 519, and 481 m^3 s^{-1}, respectively. While there is a great deal of surface water to the west, south, and east of the Montezuma Hills appraisal well site, the Montezuma Hills themselves do not contain extensive lakes or wetlands.

2.5 Subsurface

2.5.1 Introduction

A block stratigraphic column of the subsurface beneath the proposed appraisal well is shown in Figure 5. As shown, the geology appears favorable for GCS by virtue of the numerous sandstone reservoirs capped by low-permeability shale units. Critical aspects of the system relevant to leakage risk assessment discussed in this section include the properties of the ground water present, nearby natural gas resources, wells and faults as potential conduits for leakage, and the trapping that occurs in a dipping monocline absent structural closure.

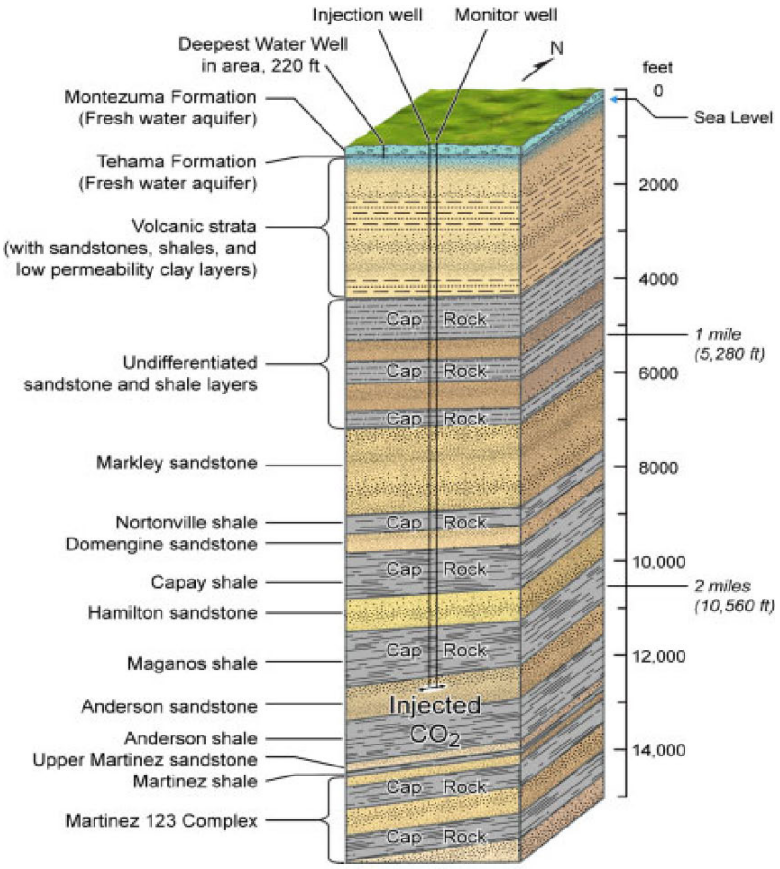

Figure 5. Block stratigraphic column of the geologic units at the appraisal well site in the Montezuma Hills.

2.5.2 Hydrology

2.5.2.1 Shallow Aquifers

Oldenburg et al. (2003) presented data on water-table elevations along with descriptions of the shallow aquifers as repeated here. As shown in Figure 6, depth to the water table varies from less than 2 m (7 ft) at lower elevations, to greater than 13 m (42 ft) around the margins of the Montezuma Hills. The greatest observed water-table depths are likely near the producing wells on the northern flanks of the Montezuma Hills.

Based on available data, the water table elevation near the center of the Montezuma Hills is about 49 m (160 ft) and decreases to about 1 m (4 ft) at the eastern edge of the hills, over a distance of about 13,700 m (45,000 ft). These values yield a maximum horizontal gradient of about 0.003. Maximum horizontal gradients from high elevations near the center of the hills to low elevations at the edges could be up to 0.01. Horizontal gradients are much less in the lowlands characterized by flat topography and perennial water channels. Water pressures are hydrostatic from the water table through the Eocene reservoirs.

The average hydraulic conductivity in the Sacramento Valley aquifer is 0.9 m d^{-1} (3 ft d^{-1}) (Williamson et al., 1989), corresponding to a permeability of approximately 10^{-12} m^2. Combining this with an estimated maximum gradient of 0.01 and an estimated effective porosity of 25% yields an estimated maximum linear groundwater velocity of 15 m yr^{-1} (50 ft yr^{-1}).

The shallow groundwater in the vicinity of the Rio Vista Gas Field has a total dissolved solids (TDS) content of 250 to 500 ppm and therefore can be characterized as fresh. Groundwater to the northwest of the Sacramento River is classified as sodium bicarbonate (Evenson, 1985; Johnson, 1985). To the southeast, the dominant chemical constituents in groundwater are sodium or calcium and chloride or sulfate (Bertoldi et al., 1991).

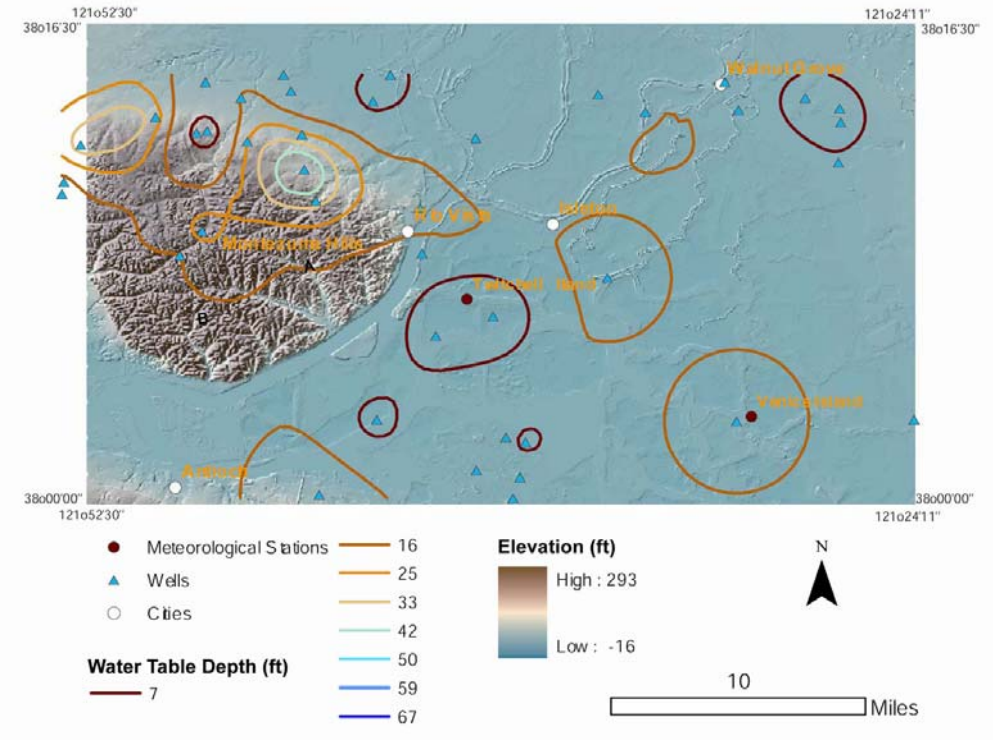

Figure 6. Water table depth and topographic elevation around the Rio Vista area.

2.5.2.2 Deep Groundwater

As described in Oldenburg et al. (2003), the base of the fresh groundwater (TDS < 2000 ppm) in the Rio Vista area generally occurs at or just below the lower contact of the Tehama Formation (Figure 5), or at a depth of 300 to 550 m (1000 to 1800 ft) below sea level (Page, 1986). The TDS of groundwater in the Markley sand at 240 m (800 ft) below sea level in the Rio Vista field is approximately 5000 ppm and the anion and cation contents are dominantly sodium and chloride, respectively, making the salinity nearly equal to the TDS. The sodium chloride content increases with depth to about 17,000 ppm in the Hamilton Sand and then decreases with depth to approximately 8000 ppm in the Peterson Sand (Johnson, 1990). This reversal in salinity (TDS) with depth was analyzed further in the preparation of this CF outline and discussion as presented further below.

The significance of TDS relates mostly to UIC regulations under the Safe Drinking Water Act, which requires non-degradation of ground water having a TDS less than 10,000 ppm. However, increasing TDS with depth (positive TDS gradient) also provides resistance to brine leakage up conduits such as wells and faults due to the higher density of the uplifted brine (e.g., Nicot et al. 2008). The TDS distribution is therefore a critical element of leakage risk assessment.

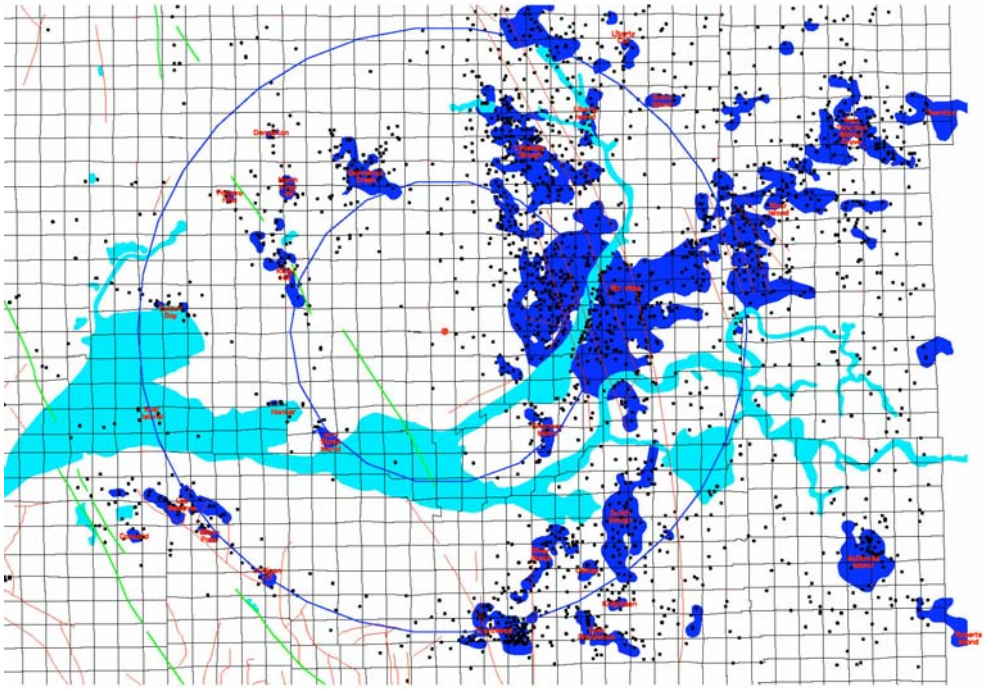

Figure 7. Gas fields surrounding the Montezuma Hills along with wells and faults.

Salinities (NaCl concentration) are shown for 36 of the 55 pools in the fields shown in Figure 7 and described in the DOGGR database (DOGGR, 19xx), while TDS values are reported for only two pools. Salinities are plotted against depth in Figure 8 with ranges shown for some of the pools. As there is no information about the distribution of the data yielding these ranges, Figure 8 plots the center of the given range within the range bars.

The two TDS (*sensu stricto*) values are also shown on Figure 8. One of these values is given for a pool along with salinity which shows that the TDS value is only slightly higher than the salinity value suggesting salinity is a reasonable proxy for TDS.

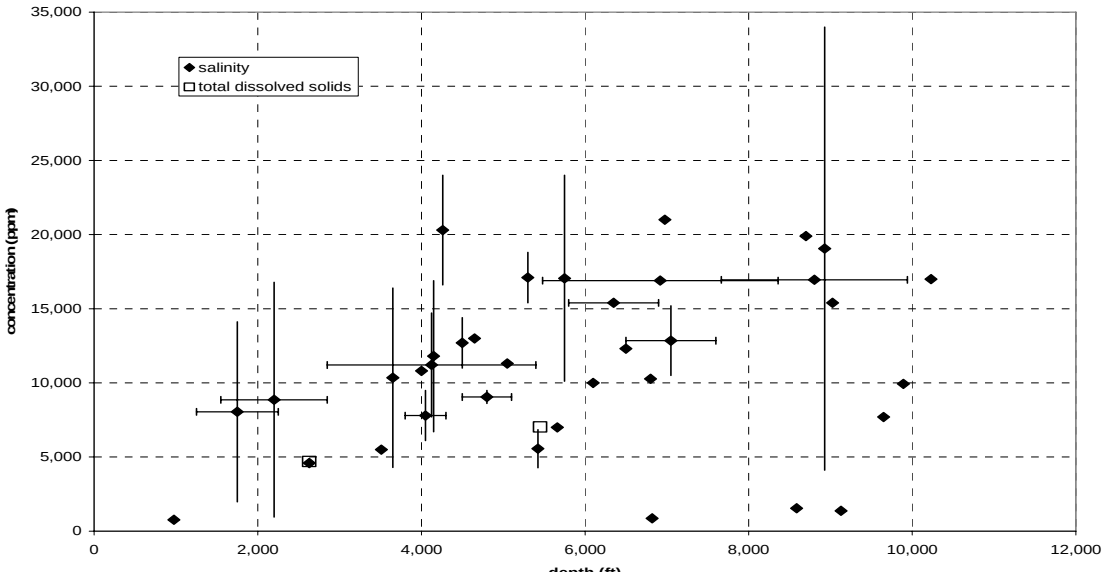

Figure 8. Total dissolved solids and salinity with depth in the natural gas pools around the FOA 15 site. Data from DOGGR ().

Salinity generally increases with depth as shown on Figure 8. A closer examination suggests the salinity gradient decreases with depth, potentially to zero or even becoming negative, below a depth of 7,000 ft (2100 m). Figure 9 shows the salinity data for each separate natural gas field. The fields are organized in the legend clockwise from north of the appraisal well site. All of the low values relative to the main trend at depths greater than 7,000 ft (2100 m) occur in fields centered generally from north to east of the site. This suggests relatively low salinities at depth are focused in this quadrant, with attendant concern for UIC non-degradation regulations, and for brine upwelling in response to storage-induced pressure rises in this area. However, there may be more widespread low-salinity water around the appraisal well site as the existing data are all for the deep pools that tend to exist only in this quadrant.

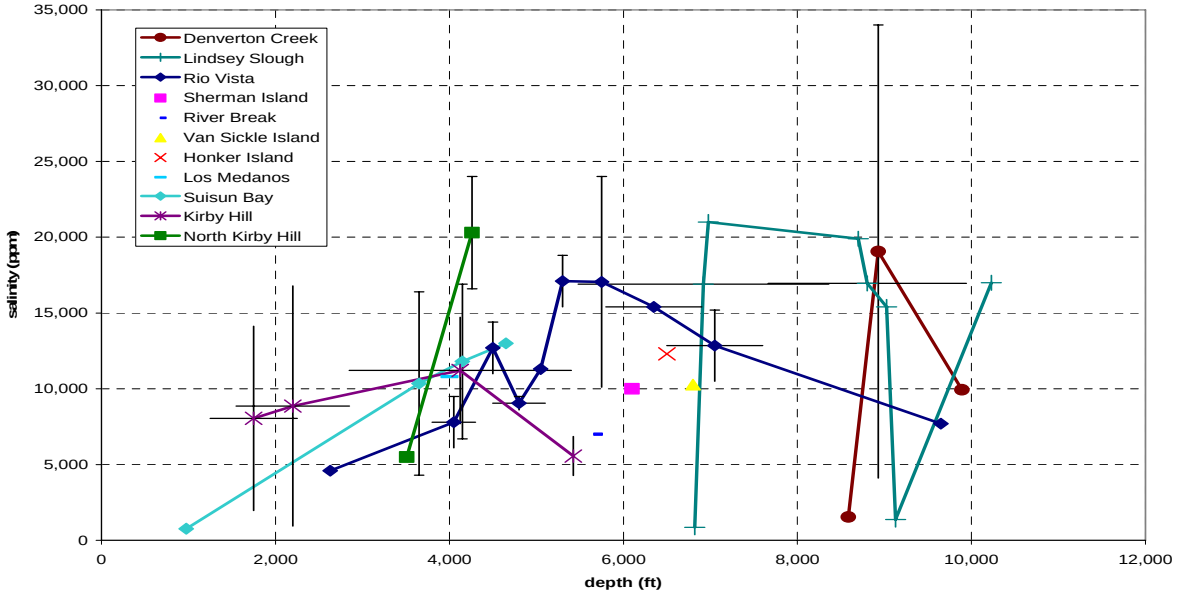

Figure 9. Salinities in natural gas pools around the FOA 15 site indicated by field.

Another perspective on salinity distribution is presented in Figure 10, which plots salinity by geologic unit. The units are listed in stratigraphic order from youngest to oldest in the legend. Salinities are available for most of the units over only limited depth ranges, although the depth range for the Domengine and Martinez is greater than 4,000 ft (1200 m). There appears to be only a slight increase in salinity with depth for the Domengine, and no increase for the Martinez. Perhaps crucially, though, the two deepest salinities for the Domengine, at about 7,000 ft (2100 m), are both slightly greater than 10,000 ppm. This, along with the slight salinity gradient in the Domengine, suggests that salinity at depths greater than 10,000 ft (3000 m) will exceed 10,000 ppm.

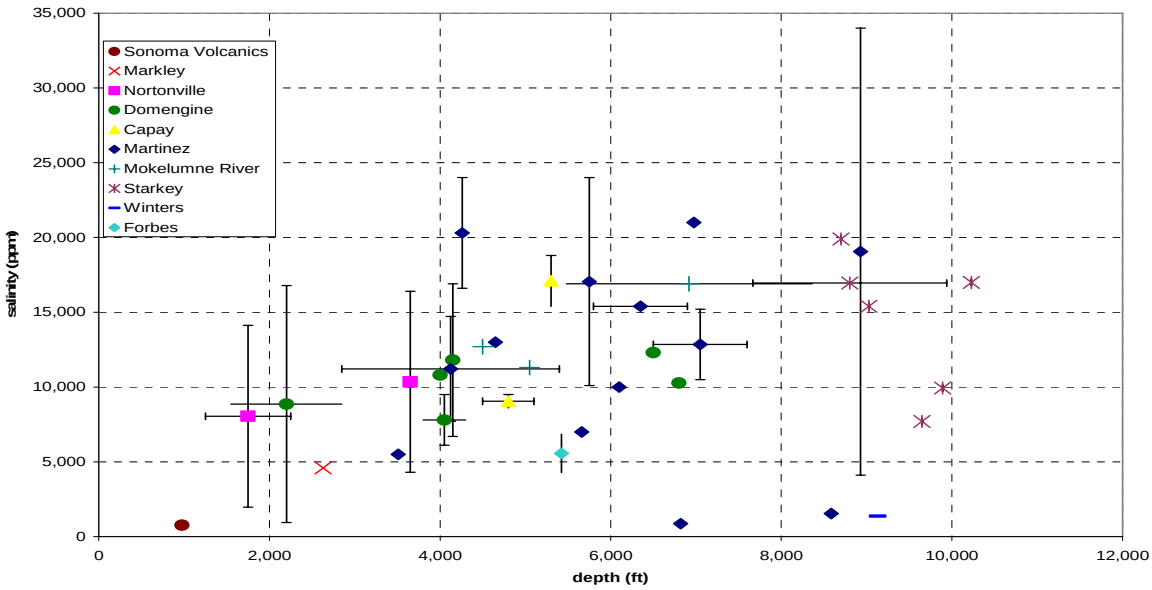

Figure 10. Salinities in natural gas pools around the FOA 15 site indicated by field.

The relative depth invariance of salinity in each geologic unit suggests aggregating the salinities in each unit. Figure 11 shows the salinity for each unit averaged from the single and range mid-point values given in Figure 10, with the range bars indicating the distribution of these points. Note the distributions for sets with more than three points (Domengine, Martinez, and Starkey) are typically platykurtic (flat relative to a normal distribution) and left skewed (more high than low values relative to a normal distribution). This indicates more probability in the tails than a normal distribution, but less probability toward the bottom of the range. Taken together, these tend to suggest somewhat normal probability at the lower end of the distribution toward the 10,000 ppm cutoff.

Figure 11 indicates increasing salinity with depth down through the section to the mid Cretaceous Forbes. There is also a fairly constant salinity gradient from the Nortonville to the Starkey, which contains the potential storage targets. Average salinities by unit are above 10,000 ppm throughout this storage section, but the bottom of the salinity distribution is below 10,000 ppm. While it is tempting to conclude from this salinity gradient, particularly as extrapolated to the deeper storage targets, that salinity will be greater than 10,000 ppm, this would be misleading. The lack of a salinity gradient or only weak salinity gradient per unit shown in Figure 10 suggests salinities in the storage targets will not be much greater than those shown on Figure 11. For instance, even though salinities at 7,700 ft (2300 m) are about 14,000 ppm using the linear trend of Nortonville to Starkey salinities, the linear trend from Domengine salinities on

Figure 10 suggests a salinity in that unit of 12,000 ppm at this depth, albeit with a distribution that likely extends below 10,000 ppm.

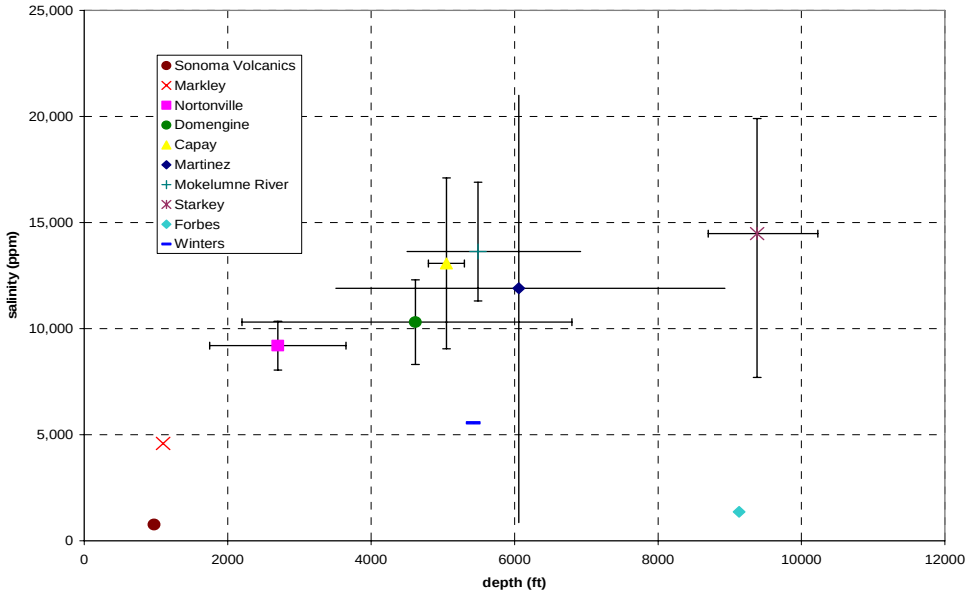

Figure 11. Salinities by geologic unit versus depth in the vicinity of the FOA 15 site.

The Mokelumne River data, at a depth shallower than the Martinez data despite the former being deeper in the section than the latter, suggests plotting the data by unit age. Figure 12 presents this perspective using approximate central ages for each unit. The salinities down through the Forbes lie on linear trend with a relatively high correlation coefficient (0.87). All of the salinities shown are below the salinity of sea water (~30,000 ppm) despite marine deposition of most of these units. This suggests deep freshwater fluid circulation at a rate higher than dissolution of cations and anions from the host rocks. Consideration should be given to the timing and possible significance of this fluid circulation relative to long term carbon storage at the site.

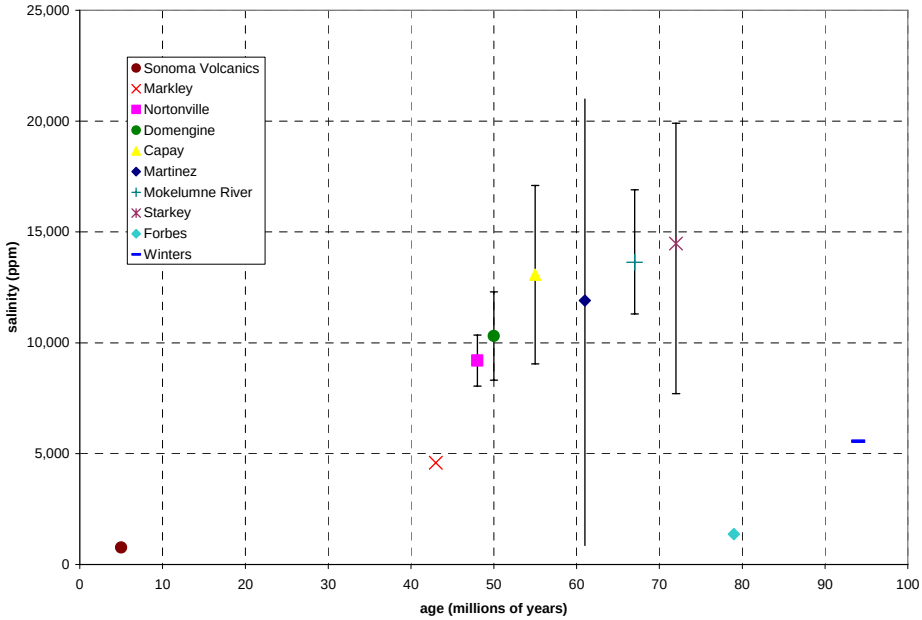

Figure 12. Salinities by geologic unit in the vicinity of the FOA 15 site.

The analysis of salinity suggests the probability that TDS in the storage targets are above the 10,000 ppm threshold is significantly greater than 50%, but less than 95%, at the storage target depths. Salinities also generally increase with depth and geologic age, but field-specific data suggest localized gradient inversion occur. The hydrostratigraphic column shown in Figure 13 represents the current understanding based on our preliminary analysis of the DOGGR data. The significance of the low TDS ground water at depth is that the system would not be at hydrostatic conditions, and that if open conduits are present there would presumably already be upwelling. Even with the general slight increase in salinity with depth, upwelling may currently be sustained over a broad area due to an overall density decrease with depth due to the geothermal gradient. Whether this is occurring or not, the low salinity gradient overall suggests pressure increases due to storage could readily induce upwelling in any leakage pathways present.

Despite the lack of a sufficient salinity gradient to significantly resist brine upwelling along potential leakage pathways in response to storage reservoir pressurization, the impact of such leakage would be significantly moderated by the low salinities involved. Because the storage target salinities are potentially very close to the 10,000 ppm threshold, significant upwelling would have to occur to significantly increase the TDS of overlying waters.

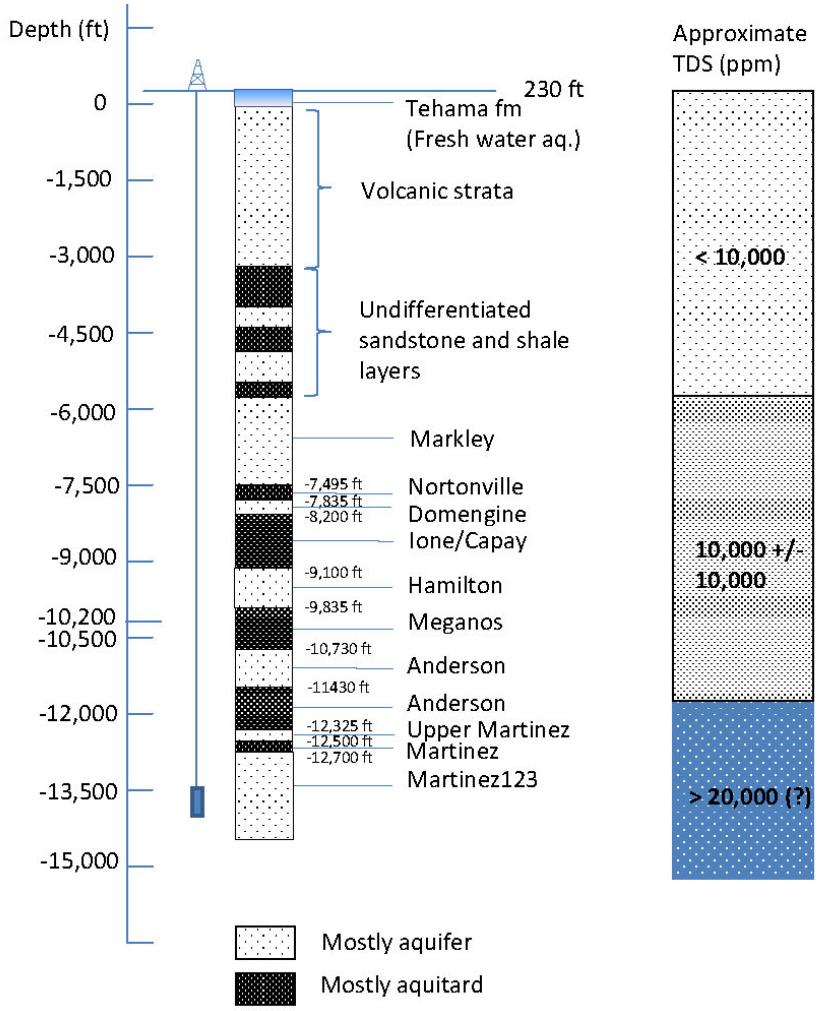

Figure 13. Expected hydrostratigraphy and water quality at the Montezuma Hills appraisal well.

2.5.3 Natural Gas Resources

Natural gas in economic quantities has not been found in the synclinal structure present at the proposed site of the Montezuma Hills appraisal well, and no gas production is noted from the Anderson or Hamilton in the DOGGR database (DOGGR, 19xx). This suggests CO_2 storage in these targets has reduced risk of impacting natural gas resources as compared to the other potential targets. However, this may be a matter of stratigraphic nomenclature, and so should be further checked and confirmed. Approximately 5 km (3 mi) to the east of the appraisal well site is the western edge of the Rio Vista Gas Field. The description below of the Rio Vista gas resource, geology, and structure repeats that given in Oldenburg et al. (2003).

The Rio Vista Gas Field is the largest onshore gas field in California (Burroughs, 1967) and has been in production since 1936. Natural gas production from the Rio Vista Gas Field peaked in 1951 with annual production of 4.4×10^9 m^3, and has declined steadily since then (Cummings, 1999). Production decline is caused by decreasing reservoir pressures and increased water production, particularly on the western boundary of the field. Cumulative production of CH_4 is in excess of 3 Tcf (9.3×10^{10} m^3) (at standard conditions of 1 bar, 15.5 ˚C [14.7 psi, 60 ˚F]).

The primary gas reservoir in the Rio Vista Gas Field is the Eocene Domengine sand, predominately a marine sandstone with shale interbeds. The Domengine resides approximately 1200 m (4000 ft) below sea level in the field area. In Figure 13, we show a highly schematic cross section (not to scale in the vertical direction) that shows the general structure of the reservoir and overlying formations. Natural gas plays have been encountered in all of the predominantly sandy formations, and in sand stringers within almost all of the predominantly shaly formations (including the Nortonville), in the Paleocene and upper Cretaceous section. Most notably, gas plays were encountered in the Markley sand above the Domengine-capping Nortonville shale. The gas traps in the Rio Vista Gas Field are described variously as faulted-dome or up-dip fault traps created by offset of reservoir sands against shales with lateral structural closure due to folding (Burroughs, 1967; Johnson, 1990).

The west-dipping Midland fault strikes northwest through the eastern portion of the Rio Vista Gas Field (Figures 7 and 13). Stratigraphic units at the reservoir level exhibit normal (down to the west) displacement, and thicken across this fault from east to west indicating syndepositional faulting. These characteristics, along with the apparent rapid accumulation of sediment and overpressuring of deeper shales led Johnson (1990) to characterize the Midland fault and associated faults as both growth and tectonic faults. Units above the Domengine sand reservoir typically exhibit reverse offset with thickening to the east indicating this fault has been tectonically reactivated in compression since the Miocene (Weber-Band, 1998). Based on regional structural analysis, Weber-Band (1998) concluded that the Midland fault and associated faults were likely due primarily to extensional tectonics during deposition of the reservoir units. West of the Midland fault, the geologic structure in the gas field consists of an elongated, faulted dome. The trend of the dome's axis and the strikes of faults cutting the dome are north to northwest. The faults appear to be sympathetic and antithetic to the Midland fault. Displacement on these faults does not appear to be greater than the thickness of the Nortonville shale, which caps the Domengine sand (see schematic cross-section Figure 13) (Burroughs, 1967; Johnson, 1990). East of the Midland fault, the gas field consists of the unfaulted half of a north- to northwest-trending elongated dome that is faulted through its eastern limb.

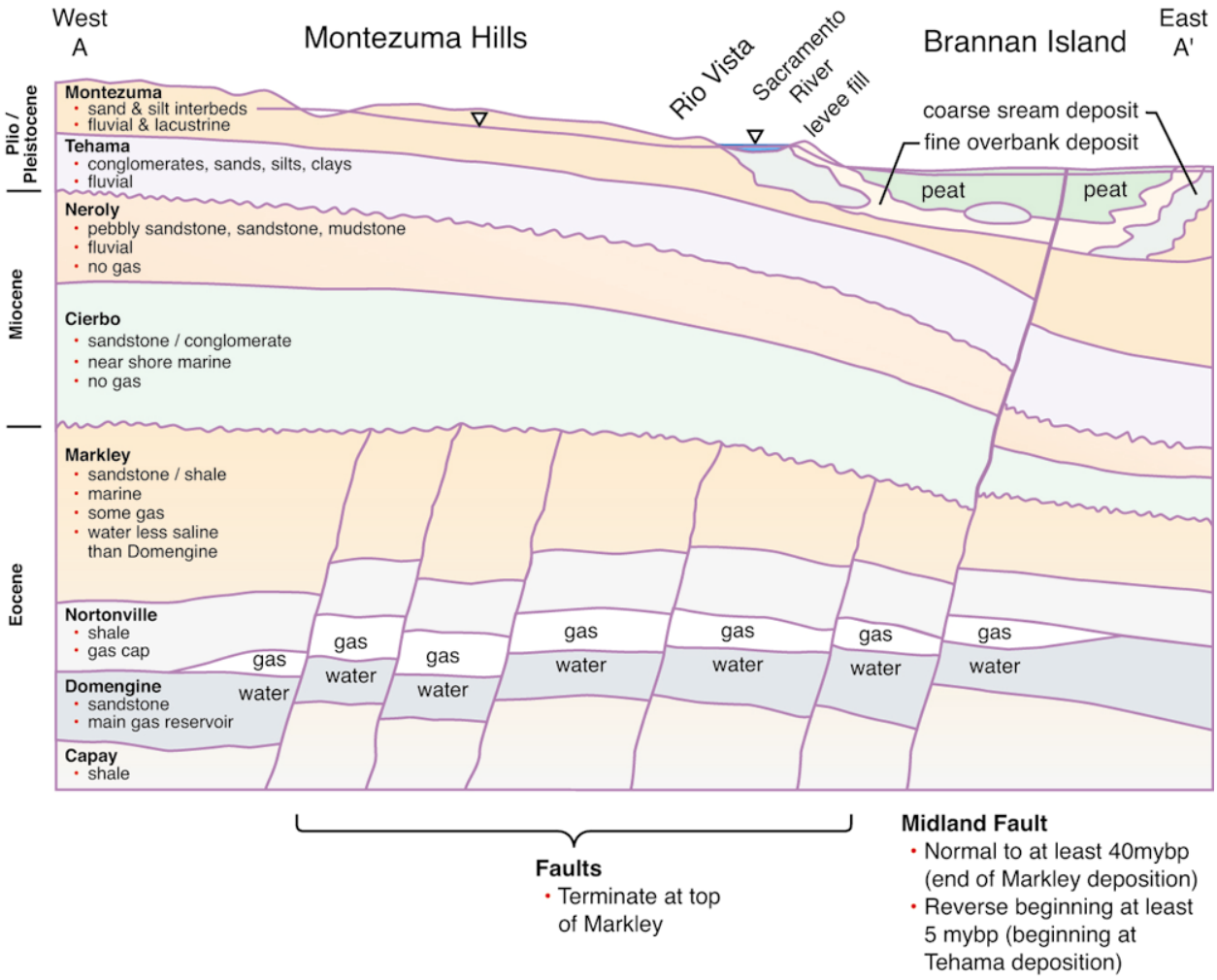

Figure 13. Cross section A-A' of the Rio Vista area from Oldenburg et al. (2003). Note that gas reservoir thickness is exaggerated relative to total formation thicknesses.

2.5.4 Geology

2.5.4.1 Montezuma Model

A three-dimensional geologic framework model needs to be developed to evaluate lithology, structure, well penetrations, and faults. Absent this model, no further discussion of the geology or structure will be presented here.

2.5.5 Boreholes

Hundreds of deep hydrocarbon (gas) exploration and production wells exist within a 20 km (12 mi) radius of the appraisal well site. Figure 14 shows existing hydrocarbon wells within and just outside of a 10 km (0.62 mi) radius of the site. Some of these wells were constructed approximately 80 years ago. Because wells are potential conduits for leakage of CO_2 and brine, the depth, current use, and integrity with respect to how well they were plugged and abandoned are critical properties for leakage risk assessment.

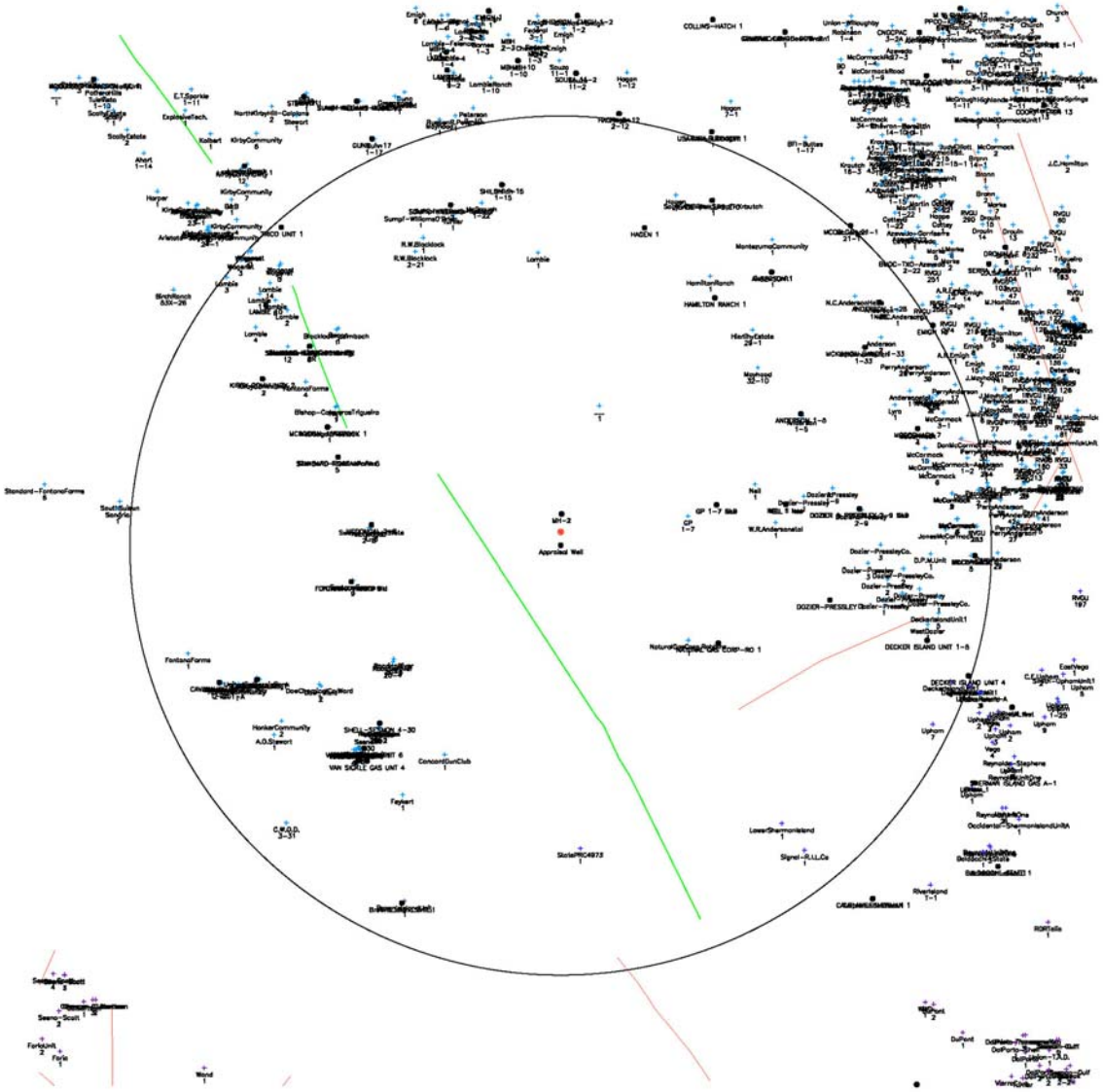

Figure 14. Approximate location of Appraisal well and possible monitoring well to the north along with 10 km (6.2 mi) circle with exploration and production wells indicated. The green line trending northwest-southeast is the Kirby Hills Fault.

2.5.6 Faults

Faults are also critical features for GCS risk assessment due to their potential for producing earthquakes and due in some cases to their potential for providing leakage pathways for CO_2 or brine. The main known faults in the area of the appraisal well are the Kirby Hills Fault (KHF) to the west and two lesser faults to the east referred to as Fault A and Fault B. The Midland Fault is a major feature to the east, just beyond the 10 km (6.2 mi) radius. A major component of ongoing research related to leakage risk will be focused on characterizing faults and their potential role as permeable pathways for CO_2 and brine. Induced seismicity and earthquake hazard is being handled by a different group working on the project.

3 References

Burroughs, E., Rio Vista Gas Field, Summary of California oil fields, 53, No. 2-Part 2, State of California, Department of Conservation, Division of Oil and Gas, 25, 1967.

California Department of Conservation, Division of Oil and Gas, Onshore oil & gas seeps in California, Publication No. TR 26, Sacramento, 1987.

Evenson, K.D., Chemical quality of groundwater in Solano and Yolo Counties, California, *United States Geological Survey Water Resources Investigations Report* 84-4244, 50 p., 1985.

Johnson, D.S., Rio Vista Gas Field--U.S.A. Sacramento Basin, California, Structural Traps III: Tectonic Fold and Fault Traps, 243-263, 1990.

Johnson, K. L., Chemical quality of ground water in Sacramento and Western Placer Counties, California; *United States Geological Survey Water Resources Investigation Report* 85-4164, 50 p., 1985.

Oldenburg, C.M., Y. Zhang, J.L. Lewicki, and P.D. Jordan, Preliminary Application of a Coupled Modeling Framework for CO_2 Leakage and Seepage at the Rio Vista Gas Field, Lawrence Berkeley National Laboratory Report LBNL-54051, October 2003.

Ota, A.Y., L.E. Schemel, S.W. Hager, and D.D. Harmon, Physical and chemical data for the Sacramento River at Rio Vista, California, November 1983 through November 1984, *United States Geological Survey Open-File Report* 86-229, 1986.

Page, R. W., 1973, Base of fresh ground water (approximately 3,000 micromhos) in the San Joaquin Valley, California, U.S. Geological Survey Hydrologic Atlas 489, 1 plate.

Page, R. W., 1986, Geology of the fresh ground-water basin of the Central Valley, California, with texture maps and sections, U.S. Geological Survey Professional Paper 1401-C, 54p. + 5 plates.

Weber-Band, J., *Neotectonics of the Sacramento-San Joaquin Delta area, east-central Coast Ranges, California*, University of California, Berkeley, doctoral thesis, 216 p., 1998.

Williamson, A. K., D. E. Prudic, and L. A. Swain, Ground-water flow in the Central Valley, California; *United States Geological Survey Profession Paper* 1401-D, 127 p., 1989.

Yielding, G., B. Freeman, and D. T. Needham, 1997, Quantitative fault seal prediction: AAPG Bulletin, v. 81, p. 897 – 917.

Zhou, W., M. Stenhouse, M. Sheppard, and F. Walton, 2004, Theme 4: Long-term risk assessment of the storage site,, in M. Wilson and M. Monea (editors), IEAGHG Weyburn CO2 monitoring and storage project summary report 2000 – 2004, p.211 – 268, Petroleum Technology Research Center, Regina, Canada.